applied sciences

MDPI

Article

Study on Energy Evolution and Damage Constitutive Model of Sandstone under Cyclic Loading and Unloading

Ji'an Luo [1,*] and Liangliang Wang [2]

[1] School of Mechanics and Photoelectric Physics, Anhui University of Science and Technology, Huainan 232001, China
[2] School of Civil Engineering and Architecture, Anhui University of Science and Technology, Huainan 232001, China
* Correspondence: fanghx@aust.edu.cn

Abstract: In order to strengthen disaster prevention control under deep resource development and space utilization, it is necessary to construct a damage intrinsic model under complex stress states to predict the mechanical behavior of deep-rock mass under cyclic loading. An indoor uniaxial cyclic loading test on sandstone was carried out in this paper. By analyzing the mechanical properties and energy transformation of the failure process, it was assumed that the failure of rock micro-units follows a Weibull density function, and the damage intrinsic relationship was constructed using the Mogi–Coulomb strength criterion. The constitutive rationality was verified via the nonlinear fitting of the experimental curve and theoretical curve, and the model parameters were analyzed. This study indicates that the cyclic loading procedure has a strengthening effect on the elastic modulus. The brittleness of the rock increases with the cycle amplitude, the axial strain accumulates continuously, and the hysteresis loop area increases gradually and moves to the right. The energy conversion of the loading process is mainly split into the energy storage phase before the damage and the release phase at the time of damage, and the dissipation energy percentage curve shows the groove evolution law. The damage intrinsic model based on the Mogi–Coulomb strength criterion accurately reflects the ontological relationship of sandstone under cyclic loading, and the model parameters have clear physical significance. This study has important theoretical and engineering meaning for predicting the deformation and destruction of rocks.

Keywords: Mogi–Coulomb strength criterion; stepped loading and unloading; damage constitutive model; sandstone damage; model parameter

check for updates

Citation: Luo, J.; Wang, L. Study on Energy Evolution and Damage Constitutive Model of Sandstone under Cyclic Loading and Unloading. *Appl. Sci.* **2023**, *13*, 1690. https://doi.org/10.3390/app13031690

Academic Editor: Ricardo Castedo

Received: 19 December 2022
Revised: 22 January 2023
Accepted: 25 January 2023
Published: 28 January 2023

Copyright: © 2023 by the authors. Licensee MDPI, Basel, Switzerland. This article is an open access article distributed under the terms and conditions of the Creative Commons Attribution (CC BY) license (https://creativecommons.org/licenses/by/4.0/).

1. Introduction

With the large-scale exploitation of shallow mineral resources in the earth, numbers are approaching exhaustion, and mineral exploitation is expanding deeper. The deep high-stress occurrence of this environment makes the rock have a mechanical behavior that is different from that of shallower depths. Traditional rock mechanics theories and methods may fail [1–4]. Moreover, with the construction of tunnels, the excavation of underground chambers and other deep underground projects, rock in its original equilibrium state is disturbed. As a result of repeated loading, the internal energy of the rock accumulates and releases, damage accumulates and the stability of the engineering of the rock is affected, thus causing a sequence of safety accidents, including rock burst and collapse. Therefore, studying the mechanical properties of deep rock during cyclic loading at different stress grades can contribute to disaster prediction and prevention.

At present, experts have conducted much research on the mechanical characteristics of rock damage and have achieved many results. There are two main methods of studying the mechanical characteristics of the rock. One is to explore the microscopic damage mechanism, and the other is to describe the macroscopic deformation behavior [5–9]. Li

et al. [10] constructed an intrinsic equation that can describe the whole stage of rock damage under the new concept of the void strain ratio, describing the relationship between rock deformation and void and skeleton deformation. Chen et al. [11] found that the Weibull probability distribution ontological model is more reasonable and superior in the plastic stage by establishing two constitutive models of rock micro-element strength, satisfying the power function distribution and Weibull probability distribution, respectively. Hu et al. [12] established an elastoplastic damage intrinsic equation considering different damages under tension and compression–shear conditions. Xie et al. [13] constructed a piecewise constitutive model based on the relationship between strain, void deformation and skeleton deformation. They believe that the rock strain before the rock yield can be composed of void strain and skeleton strain.

According to the laws of thermodynamics, material destruction is accompanied by energy transformation [14,15]. Meng et al. [16] investigated the energy properties of limestone under different confining pressures. Wu et al. [17] established a nonlinear relationship between different energy characteristics of granite and cycle amplitude and cycle times. Li et al. [18] performed comparative research of rock energy under different moisture contents.

In summary, it is hard to represent rock changes under complex stress states by using the damage intrinsic relation of conventional M-C and D-P theory. Based on this, a damage intrinsic model considering the effect of intermediate principal stress can be established. The strength of the rock micro-units satisfies the Mogi–Coulomb strength criterion, and the micro-units failure follows the Weibull probability formula. The constitutive model with fewer parameters can be combined with the nonlinear fitting function of the Origin software to obtain the model parameters quickly. It is more suitable to analyze internal changes in the deep underground surrounding rock. In this paper, the model verification and model parameter analysis were carried out through a cyclic loading test on sandstone. The law of mechanical parameters and the energy in the course of cyclic loading are explored, and the damage properties of sandstone under high-stress cyclic loading were revealed, which provides some theoretical support for underground engineering.

2. Sandstone Sample Preparation and Testing Process

A total of six standard cylindrical specimens with a diameter of 50 mm and a height of 100 mm were made according to the recommendations of the International Society of Rock Mechanics, and the error of non-parallelism at both ends of the specimens was not more than ± 0.05 mm. The shape of the specimen is shown in Figure 1.

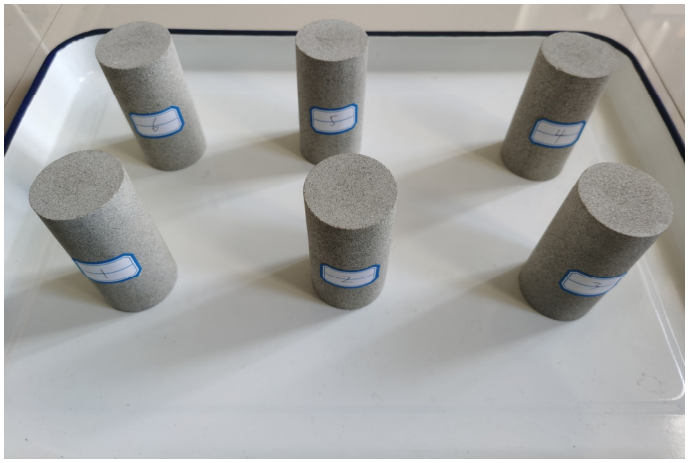


Figure 1. Rock specimen.

The adopted test was the cyclic loading test. The sandstone cyclic loading tester is shown in Figure 2. First, according to the uniaxial compression test of sandstone, the unconfined uniaxial compressive strength of sandstone was determined to be 87.6 MPa.

The cyclic loading test was divided into seven amplitudes, namely 30, 40, 50, 60, 70, 80 and 90 MPa, and the loading and unloading rate was 0.5 kN/s. Each cycle was loaded at a set rate to a specified value and was then unloaded to 0 MPa at the same rate, and six cycles of cyclic loading tests were performed in turn until the specimen was damaged. The specific circulation method is shown in Figure 3.



Figure 2. Sandstone cyclic loading tester.

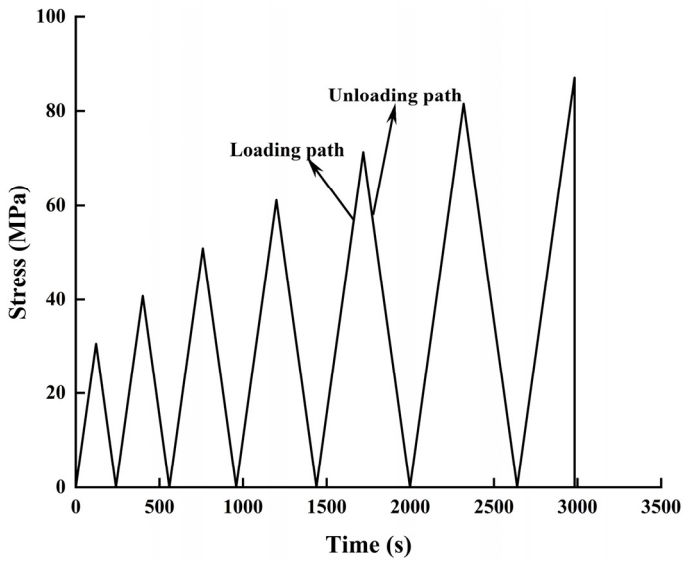


Figure 3. Circulation method.

3. Test Curve Analysis

In order to simulate the disturbance effect of engineering instruments on sandstone, a cyclic loading test was designed. The sample test curve under cyclic loading is shown in Figure 4. Under repeated cyclic loading, the loading curve rises roughly along the loading path parallel to the previous grade, showing an obvious rock deformation memory phenomenon [19–22]. In the course of cyclic loading, the damage of sandstone accumulated continuously, the internal cracks extended continuously, the axial strain increased continuously, the test curves of cyclic loading moved forward continuously and the concave degree increased continuously. At the peak load of the seventh cycle, the rock curve dropped sharply, and the sandstone suddenly lost its carrying capacity.

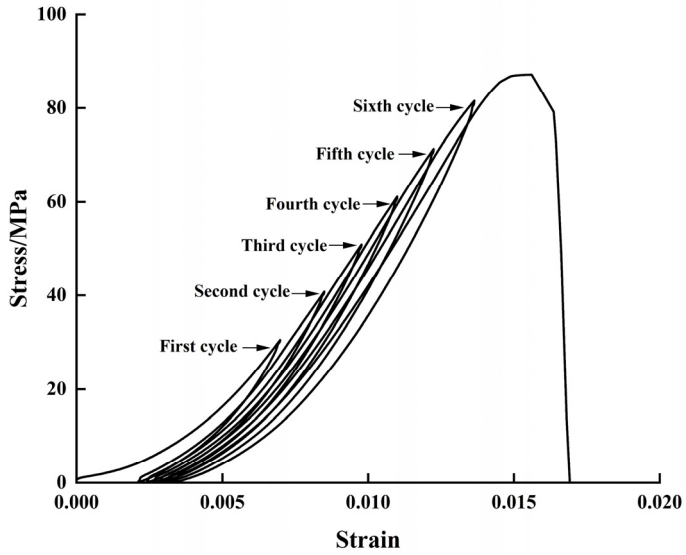


Figure 4. Sandstone cyclic loading test curve.

3.1. Elastic Modulus and Axial Strain

As an important mechanical parameter of rock, the elastic modulus highlights the brittle characteristics of the rock. The elastic modulus under cyclic loading can be obtained from a single cyclic loading curve [23]. In this paper, the elastic modulus of each cycle level was calculated using the peak value of the loading curve and the minimum value of the unloading curve. According to the mechanical indexes of sandstone under different upper limit stresses, as shown in Figure 5, the internal void cracks of sandstone were continuously compacted under the load, and the elastic modulus of rock increased continuously, which could be roughly divided into two stages: rapid growth and stability. As the elastic modulus of rock increased, the brittleness of rock gradually increased until the final unstable failure of the rock.

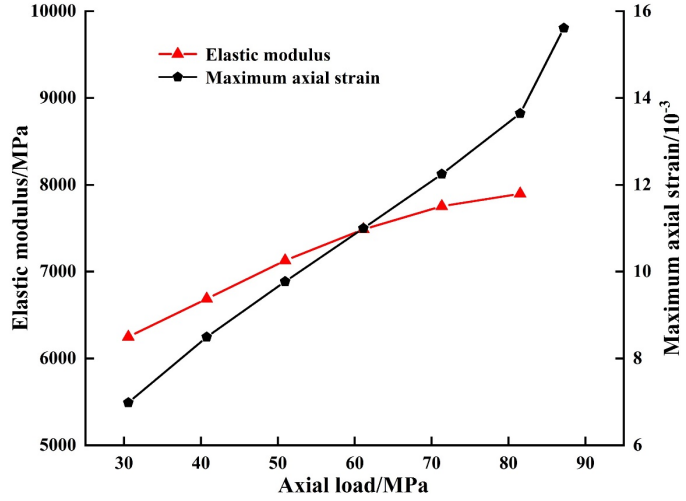


Figure 5. Mechanical indexes at different upper stresses.

Figure 5 also shows that, owing to the strengthening effect of repeated cyclic loading, the friction of rock particles in the crack section was more intense. During the period loading course of the rock, the damage accumulated continuously, and the axial strain increased continuously until the post-peak stage of rock failure reached the maximum.

3.2. Energy Characteristics

The cyclic loading process is accompanied by the input and output of energy. The energy input during the loading process is partly used for the storage of rock elastic energy and is partly dissipated due to the development of damage inside the rock. The relationship among the three can be obtained according to the first theorem of thermodynamics [24–26].

$$U = U_e + U_d \tag{1}$$

$$U_e = \int_{\varepsilon_1}^{\varepsilon_2} \sigma d\varepsilon \tag{2}$$

$$U_d = \int_0^{\varepsilon_1} \sigma d\varepsilon - \int_{\varepsilon_1}^{\varepsilon_2} \sigma d\varepsilon \tag{3}$$

where U is the total input energy density, U_e is the elastic energy density and U_d is the dissipation energy density.

According to the diagram's expression of the relationship between energy density values in Figure 6, the elastic deformation energy stored in the rock unloading process was released. The area under the unloading curve and the strain axis is the elastic energy density. According to the relationship between fracture mechanics and energy, the area enclosed by the loading curve and unloading curve is the dissipated energy density. Dissipation energy consists of friction energy dissipation and crushing energy dissipation [27], which causes the accumulation of rock internal damage, crack initiation and propagation, and the formation of a sharp leaf-like hysteresis loop between the upper unloading curve and the lower loading curve due to the multi-phase, multi-component and non-uniformity characteristics of the rock.

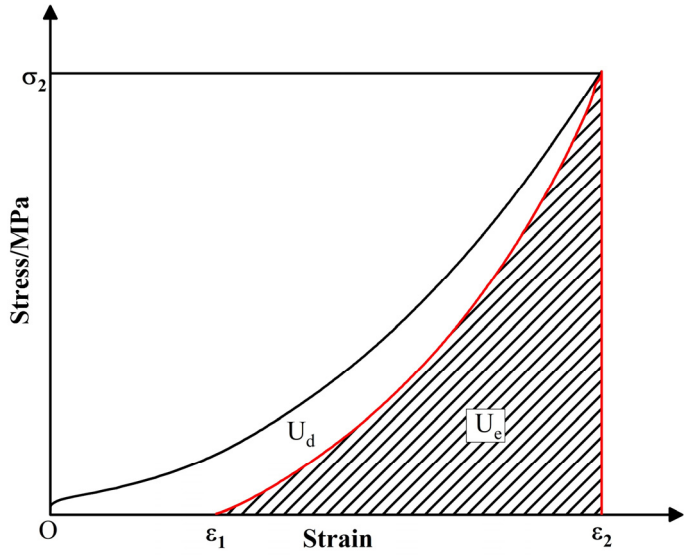


Figure 6. Rock energy density value relationship diagram.

Energy conversion was used to further analyze the damage process inside the rock under different cycle amplitudes. The results are shown in Figure 7. The analysis suggests that the energy transformation process under cyclic loading can be divided into four stages: the compaction stage, elastic stage, plastic stage and failure stage. The curve of the dissipation energy percentage and elastic energy percentage shows obvious groove and inverted groove evolution. In the compaction stage, due to the compaction of pores and cracks in the rock, the percentage of dissipated energy in the input energy was large, but in the compaction stage, the elastic stage and the plastic stage were still dominated by elastic energy storage. In the plastic stage, due to the increase in the unrecoverable plastic strain of the rock, the elastic energy of the rock decreased by 1.86%, and the dissipation energy increased by 1.86%. In the failure phase, the elastic energy of the rock was released, and the

dissipation energy increased rapidly, resulting in the loss of the carrying stability of the rock. From an energy point of view, the sudden release of the elastic energy accumulated inside the rock was the internal cause and power source of rock failure.

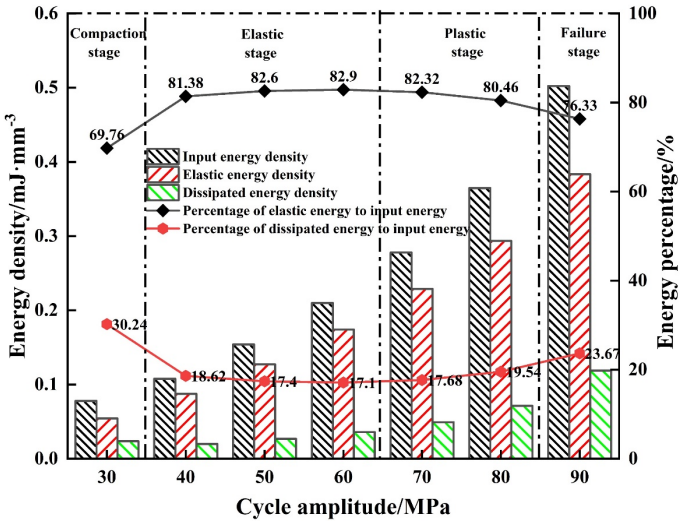


Figure 7. Energy transformation during the cyclic loading process.

Figure 8 shows the hysteresis loop contours and the hysteresis energy density–cycle amplitude relationship curve. The analysis shows that, as the amplitude of the cycles increased, the plastic damage of the rock increased continuously, the hysteresis loop moved to the right, the area increased continuously and the hysteresis curve of the rock changed from dense to sparse. The nonlinear data fitting of the rock hysteresis energy density and cycle amplitude was carried out. The fitting results are as follows:

$$y = -0.018 + 0.0096e^{\frac{x}{49.10}} \quad (4)$$

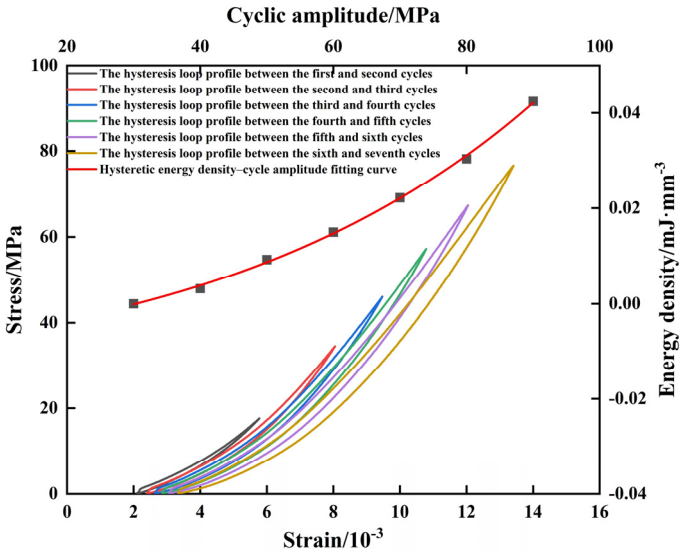


Figure 8. Hysteretic loop profile and hysteretic energy density–cycle amplitude relationship curve.

4. Establishment of the Constitutive Model

4.1. Establishment of the Damage Constitutive Relation

The damage intrinsic relation is based on the strain equivalence hypothesis proposed by Lemaitre [28], as follows:

$$[\sigma^*] = [\sigma]/(1-D) = [E][\varepsilon^e]/(1-D), \tag{5}$$

where $[\sigma^*]$ is the effective stress matrix; $[\sigma]$ is the nominal stress matrix; $[E]$ is the elastic matrix of the material; $[\varepsilon^e]$ is the elastic strain matrix; and D is the damage variable.

Due to the internal defects of the rock itself and many influencing factors in the procedure of rock damage, the determination of the damage variables has always been a top priority in the study of rock mechanics. According to different methods, the selection of damage variables in different research directions is different. Based on the method adopted by Cao et al. [29–31], this paper introduces two assumptions: the strength of the micro-units satisfies the Weibull probability formula and the macroscopic isotropic of rock materials. The formula for the rock failure criterion is assumed to be

$$f(\sigma^*) = k_0, \tag{6}$$

where k_0 is the constant of material cohesion related to the internal friction angle. In line with the probability principle, the probability of the rock micro-unit strength failure is

$$P[f(\sigma^*)] = P[k_0]. \tag{7}$$

The probability of the damage variable is

$$D = \int_0^{k_0} G(x)dx, \tag{8}$$

where: $G(x)$ is the Weibull probability distribution.

4.2. Establishment of Rock Micro-Element Strength

Rock failure, according to the principles of calculus, is a macroscopic manifestation of the strength failure of a large number of rock micro-elements. When any principal stress on the rock reaches the yield strength of the rock, rock failure occurs. Most studies [32] suggest that there is a threshold value when the intermediate primary stress σ_2 increases. When it is less than the threshold value, the rock strength increases with the increase in the intermediate principal stress. When the intermediate primary stress surpasses the threshold value, the strength starts to decline. There are also related studies [33,34] in which, by keeping σ_1 and σ_3 unchanged, σ_2 alone can lead to rock failure. However, the Mohr–Coulomb and Griffith single shear theories lack the consideration of intermediate principal stress, σ_2, and it is difficult to express the state of rock mechanics in complex states. Based on a large number of triaxial tests, Mogi et al. [35,36] considered the function of the intermediate principal stress σ_2 and believed that the brittle fracture of the material occurs in a plane parallel to the σ_2 direction, and the distortion energy inside the material reaches the limit value. The failure of the yield surface depends on the effective intermediate stress, σ_{ef}, rather than the average effective stress, σ_{ave}.

$$\sigma_{ave} = (\sigma_1 + \sigma_2 + \sigma_3)/3 \tag{9}$$

The Mogi–Coulomb rock strength theory can better describe the unloading failure characteristics under high-stress states. Therefore, the Mogi–Coulomb rock strength criterion is introduced in this paper, and the octahedral stress is expressed as a function of the effective intermediate stress [37], as follows:

$$\tau_{oss} = \alpha + \beta\sigma_{ef} \tag{10}$$

$$\tau_{oss} = \frac{1}{3}\sqrt{(\sigma_1 - \sigma_2)^2 + (\sigma_2 - \sigma_3)^2 + (\sigma_3 - \sigma_1)^2} \tag{11}$$

$$\sigma_{ef} = \frac{\sigma_1 + \sigma_3}{2}, \tag{12}$$

where τ_{oss} is the octahedral shear stress, α, β are material parameters related to the rock's mechanical characteristics and σ_{ef} is the effective intermediate stress. Under the conventional triaxial condition, the Mogi–Coulomb rock strength criterion degenerates into the Mohr–Coulomb criterion relation, and then the following is obtained:

$$\alpha = \frac{2\sqrt{2}}{3} c \cos\varphi \tag{13}$$

$$\beta = \frac{2\sqrt{2}}{3} \sin\varphi, \tag{14}$$

where c is the cohesion and φ is the internal friction angle.

Therefore, the micro-unit strength, considering damage based on the Mogi–Coulomb strength formula, can be expressed as

$$\lambda = \alpha + \beta \cdot \frac{\sigma_1^* + \sigma_3^*}{2}, \tag{15}$$

where λ is the distribution variable of micro-unit strength failure.

4.3. Establishment of Triaxial Constitutive Relation

Assuming that the damage of the rock material's micro-units satisfies the Weibull probability distribution, the probability density distribution function of rock can be expressed as

$$G(\lambda) = (\frac{m}{\lambda_0})(\frac{\lambda}{\lambda_0})^{m-1} \exp[-(\frac{\lambda}{\lambda_0})^m], \tag{16}$$

where m and λ_0 are Weibull distribution parameters.

The damage variable obtained by substituting Equation (16) into Equation (8) yields

$$D = \int_0^{\lambda} G(x)dx = 1 - \exp[-(\frac{\lambda}{\lambda_0})^m]. \tag{17}$$

The general form of the generalized Hooke law and the Lemaitre strain equivalence assumption is as follows:

$$\varepsilon_i = \frac{1}{E}[\sigma_i^* - \mu(\sigma_j^* + \sigma_k^*)](i, j, k = 1, 2, 3), \tag{18}$$

where E is the elastic modulus and μ is the Poisson ratio.

$$\sigma_i^* = \frac{\sigma_i}{1 - D}(i = 1, 2, 3) \tag{19}$$

Using Equation (19), the damage relation of the rock under triaxial action can be obtained, as follows:

$$\sigma_1 = [E\varepsilon_1 + \mu(\sigma_2^* + \sigma_3^*)] \exp[-(\frac{\lambda}{\lambda_0})^m] = [E\varepsilon_1 + \mu(\sigma_2^* + \sigma_3^*)] \exp[-[(\alpha + \beta \cdot \frac{\sigma_1^* + \sigma_3^*}{2})/\lambda_0]^m] \tag{20}$$

$$\sigma_1 = E\varepsilon_1(1 - D) + \mu(\sigma_2 + \sigma_3) \tag{21}$$

or

$$\sigma_1 = E\varepsilon_1 \cdot \exp[-[(\alpha + \beta \cdot \frac{\sigma_1^* + \sigma_3^*}{2})/\lambda_0]^m] + \mu(\sigma_2 + \sigma_3). \tag{22}$$

In summary, from Equation (22), the rock uniaxial constitutive model is

$$\sigma_1 = E\varepsilon_1 \exp[-[(\alpha + \beta \cdot \frac{1+\mu}{2} \cdot E\varepsilon_1)/\lambda_0]^m]. \quad (23)$$

4.4. Model Validation

In the past, most of the verification of Mogi–Coulomb criterion has been based on loading conditions, but it has been less focused on the verification of both loading and unloading conditions. In this validation, in order to prevent the over-parameterization of the intrinsic equation in the fitting process and the failure of the fitting, Equation (23) is transformed, and the equivalent constitutive equation is constructed using $A = \alpha$ and $B = \beta \cdot \frac{1+\mu}{2}$.

$$\sigma_1 = E\varepsilon_1 \exp[-((A + B \cdot E\varepsilon_1)/\lambda_0)^m] \quad (24)$$

In the process of model validation, the basic physical parameters of the rock are as follows: φ is 45.42° and c is 10.02 MPa. When the data fitting effect of Equation (24) is better, the rationality of the intrinsic model can be confirmed. First, according to the cyclic loading test, the loading and unloading test curves under each cycle amplitude were obtained. Then, using the nonlinear fitting function of the Origin software, combined with the model relationship (24), a new custom fitting function was established with m and λ_0 as parameters. The applicability of the model's establishment was quickly determined according to the fitting correction coefficient R^2 through the rapid iteration of the Levenberg–Marquardt method embedded in the software. The fitting curves of the loading stage amplitudes of 30 MPa and 90 MPa and the unloading stage amplitudes of 30 MPa and 80 MPa were randomly selected and compared with the test curves. The comparison results are shown in Figures 9 and 10.

As shown in Figures 9–11, except for some deviations in the initial stage, the fitting degree between the theoretical curve and the experimental curve is high. According to the fitting parameters of each cycle level in Table 1, the fitting correction coefficient R^2 of the fitting curve of the test data is above 0.99, which also shows that the rock intrinsic relationship has good applicability and rationality. According to the comparison between the loading phase and the unloading phase, the fitting effect of the loading section was better than that of the unloading section. Moreover, the fitting effect of loading and unloading curves with different amplitudes was compared. With the continuous accumulation of rock damage, the fitting effect of the rock test curve is better.

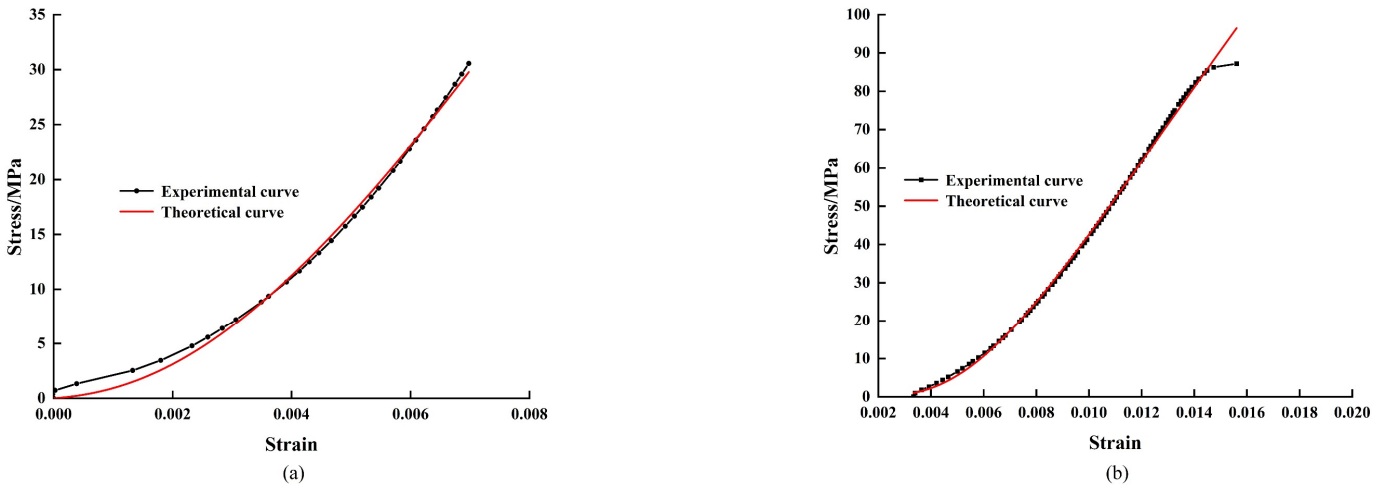


Figure 9. Curve fitting of loading section: (**a**) 30 MPa. (**b**) 90 MPa.

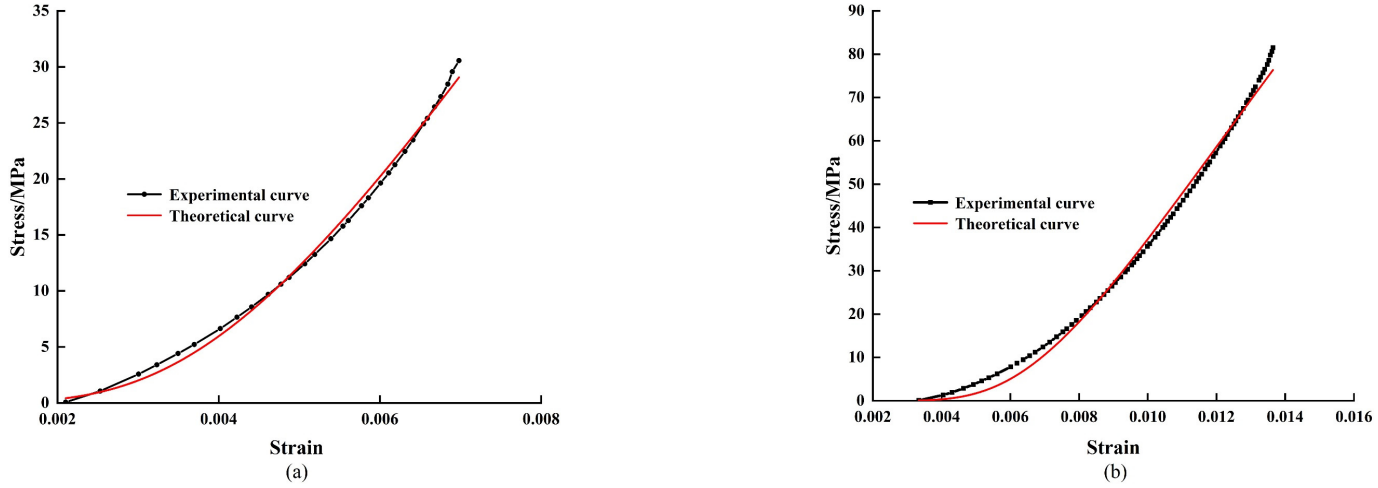


Figure 10. Unloading curve fitting: (**a**) 30 MPa. (**b**) 80 MPa.

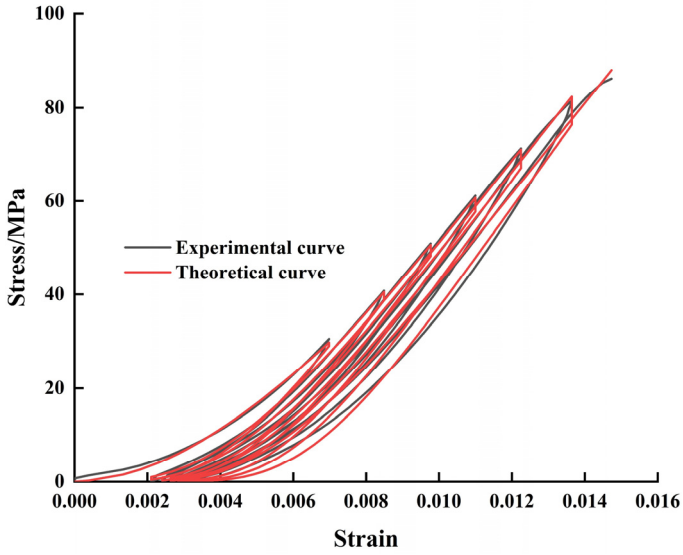


Figure 11. Experimental curve fitting of whole-stage cyclic loading process.

Table 1. Fitting parameters of each cycle.

Loading or Unloading	Amplitude/MPa	λ_0/MPa	m	R^2
Loading	30	24.940	−1.767	0.997
	40	28.451	−2.629	0.999
	50	29.804	−2.822	0.998
	60	30.947	−2.938	0.998
	70	32.004	−2.998	0.998
	80	33.148	−3.007	0.999
	90	34.446	−2.800	0.997
Unloading	30	28.483	−3.285	0.996
	40	30.854	−3.401	0.995
	50	32.470	−3.475	0.995
	60	33.996	−3.551	0.994
	70	35.580	−3.553	0.994
	80	37.603	−3.477	0.994

Through the observation of Table 1, the constitutive parameters λ_0 and m of the rock in the loading section are smaller than those in the unloading section under different cycle amplitudes. In the first five loading–unloading processes, the parameter λ_0 is proportional

to the loading–unloading amplitude, and the parameter m is inversely proportional to the loading–unloading amplitude. The m value of the rock increases slightly under the sixth and seventh cyclic loading–unloading in the rock, approaching the failure stage. The relationship between parameters λ_0, m and the amplitude are shown in Figure 12.

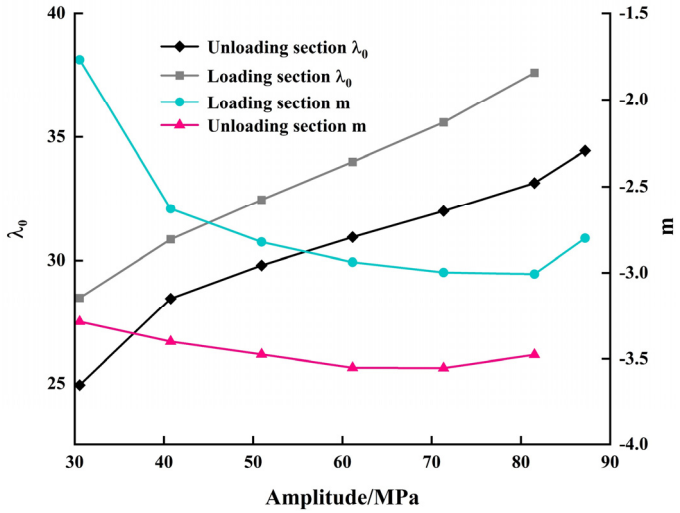


Figure 12. Relationship between parameters λ_0, m and amplitude.

5. Parameter Study

In the above tests of different loading and unloading sections of sandstone, the Levenberg–Marquardt (L–M) method embedded in the nonlinear fitting function of Origin software was used to select the iteration with initial values of the appropriate parameters such that the residual error between the fitting function (24) and the test data was minimized and the specific values of parameters m and λ_0 were obtained. It was found that parameters λ_0 and m have certain rules. Therefore, the degree of influence and the physical significance of constitutive parameters λ_0 and m on the theoretical curve of the constitutive graded loading–unloading were determined via parametric studies.

5.1. Parameter m Study

Taking the first-stage loading as an example, the fixed parameter λ_0 value was 24.940, and the values of m were -1, -1.5, -2 and -2.5. The study results of parameter m are shown in Figure 13. When the stress level is less than 11 MPa, the theoretical curve decreases with the m value, and the concave degree of the curve increases continuously. Due to the large number of initial voids and cracks in the rock, the initial damage was large, and the strain should have been changed greatly under an equal stress grade. When the stress grade is greater than 11 MPa, the theoretical curve of the rock is steeper with decreases in the value of m. According to the steepness of the curve, as the curve becomes steeper, the elastic modulus becomes greater, the stiffness of the rock becomes greater, and its brittleness becomes greater. It was easy to determine the value of m, which controls the degree of brittleness of the rock. Under the same stress level, as the m value becomes smaller, the rock strain becomes greater, and the initial damage becomes greater. Under the action of cyclic stress, most of the work done by the initial stress of the rock acts on the initial damage compaction stage, and less work is done for the extension and expansion of rock cracks. Under the same external force, the total amount and growth rate of rock cracks decrease. Compared with the larger m value, the initial damage of the rock is smaller, the stress works earlier on crack propagation, and the cumulative number of cracks in the rock is larger. Therefore, it can be inferred that the level of m reflects the degree of crack propagation. As the degree of rock fracture propagation becomes greater, the level of m becomes greater. According to the physical meaning of the value of m, because the loading–unloading process of the sixth and seventh cycles approaches the rock failure

stage, rock fracture extends and expands to a large extent, and its effect on the increase in the level of m exceeds the effect of the initial damage of the rock on the reduction in the level of m. The phenomenon of slight increases in m is also explained.

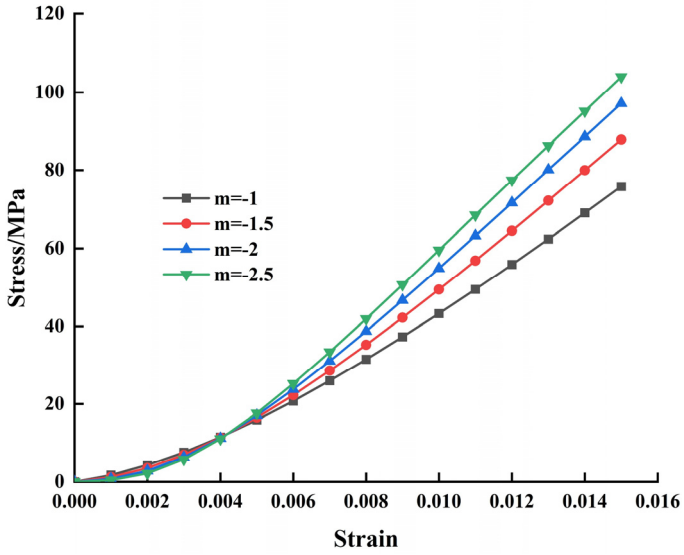


Figure 13. Parameter m study.

5.2. Parameter λ_0 Study

Similarly, taking the first-stage loading as an example, the fixed parameter m was -1.767, and the λ_0 values were 20, 25, 30 and 35. The study results of parameter λ_0 are displayed in Figure 14. As can be observed, the shapes of the theoretical curves under different λ_0 values are generally similar. With increases in the value of λ_0, the peak strength of the curve decreases continuously, and the curve becomes flatter. It is easy to conclude that parameter λ_0 has an important impact on the average macroscopic strength of the rock.

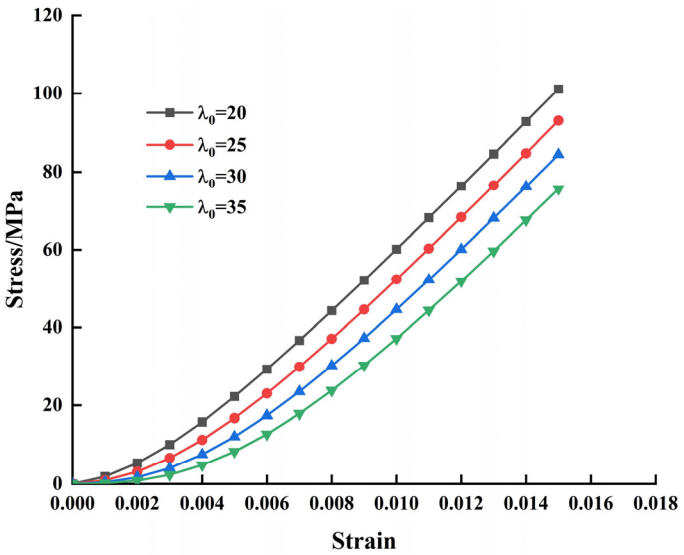


Figure 14. Parameter λ_0 study.

6. Conclusions

(1) Under cyclic loading, the elastic modulus is proportional to the cycle amplitude. During the cyclic loading process, cracks continue to expand, axial strain continues to increase, and rock damage continues to accumulate.

(2) Under the action of cyclic loading, the elastic energy of sandstone accumulates continuously. In the damage stage, the percentage of dissipated energy increases obviously, and the percentage curve shows obvious groove evolution characteristics. The hysteresis energy density gradually increases with the cycle amplitude, and the hysteresis curve changes from dense to sparse, constantly moving toward the direction of strain increase.

(3) A damage intrinsic model based on the Mogi–Coulomb rock strength criterion is established, which can accurately reflect the ontological relationship of sandstone under cyclic loading.

(4) The influence of parameters on the theoretical curve and its physical meaning are determined. Parameter λ_0 is related to the average macroscopic strength of the rock. As parameter λ_0 becomes larger, the theoretical curve becomes smoother, and the average macroscopic strength of the rock becomes smaller. Parameter m is related to the initial damage, degree of brittleness and degree of crack extension. As parameter m becomes larger, the concave degree of the theoretical curve is becomes smaller, the initial damage of the rock becomes smaller, the degree of brittleness becomes smaller, and the degree of crack extension becomes larger.

Author Contributions: Conceptualization, J.L.; formal analysis, J.L. and L.W.; data curation, J.L.; writing—original draft preparation, J.L. and L.W.; writing—review and editing, J.L. and L.W.; supervision, J.L. The results were discussed and the conclusions drafted jointly by all authors. All authors have read and agreed to the published version of the manuscript.

Funding: This research was funded by the Anhui University Natural Science Foundation (KJ2021A0424); State Key Laboratory Program (SKLGDUEK1212); Quality Engineering Project of Anhui Provincial Department of Education (2016zy039, 2020zyrc054).

Institutional Review Board Statement: Not applicable.

Informed Consent Statement: Not applicable.

Data Availability Statement: Not applicable.

Acknowledgments: The authors thank the anonymous reviewers for their careful review, contributions and criticism, which help with the improvement of the manuscript. The authors are indebted to Zhixi Liu and Jun He of Anhui University of Science and Technology for their great help in performing the tests.

Conflicts of Interest: The authors declare no conflict of interest.

References

1. Zhang, Z.Y.; Wang, J.G.; Huang, Y.H.; Li, X.L.; Zhao, W. Experimental analysis on dynamic characteristics and failure mode of deep dolomite based on high-speed photography. *Chin. J. Undergr. Space Eng.* **2018**, *14*, 1195–1201.
2. Gao, M.Z.; Ye, S.Q.; Yang, B.G.; Liu, Y.T.; Li, J.H.; Liu, J.J.; Xie, H.P. Progress in research on deep in situ rock mechanics. *Bull. Natl. Nat. Sci. Found. China* **2021**, *35*, 895–903.
3. Askaripour, M.; Saeidi, A.; Rouleau, A.; Mercier-Langevin, P. Rockburst in underground excavations: A review of mechanism, classification, and prediction methods. *Undergr. Space* **2022**, *7*, 577–607. [CrossRef]
4. Lippmann-Pipke, J.; Erzinger, J.; Zimmer, M.; Kujawa, C.; Boettcher, M.; Heerden, E.V.; Bester, A.; Moller, H.; Stroncik, N.A.; Reches, Z. Geogas transport in fractured hard rock—Correlations with mining seismicity at 3.54Km depth, TauTona gold mine, South Africa. *Appl. Geochem.* **2011**, *26*, 2134–2146. [CrossRef]
5. Xu, X.L.; Murat, K.; Gao, F.; Zhang, Z.Z. Thermal damage constitutive model for rock considering damage threshold and residual strength. *J. Cent. South Univ.* **2018**, *25*, 2523–2536. [CrossRef]
6. Jiang, H.P.; Jiang, A.N.; Yang, X.R. Statistical damage constitutive model of high temperature rock based on Weibull distribution and its verification. *Rock Soil Mech.* **2021**, *42*, 1894–1902.
7. Li, H.C.; Zhang, S. A constitutive damage model of rock based on the assumption of modified Lemaitre strain equivalence hypothesis. *Rock Soil Mech.* **2017**, *38*, 1321–1326+1334.
8. Sun, M.C.; Xu, W.Y.; Wang, S.S.; Wang, R.B.; Wang, W. Study on damage constitutive model of rock based on principle of minimum dissipative energy. *J. Cent. South Univ. (Sci. Technol.)* **2018**, *49*, 2067–2075.
9. Xie, S.J.; Han, Z.Y.; Hu, H.H.; Lin, H. Application of a novel constitutive model to evaluate the shear deformation of discontinuity. *Eng. Geol.* **2022**, *304*, 106693. [CrossRef]

10. Li, X.L.; Chen, H.K.; Zhang, J.H. Statistical damage model for whole deformation and failure process of rock considering initial void closure. *J. Southwest Jiaotong Univ.* **2022**, *57*, 314–321.
11. Chen, S.; Qiao, C.S.; Ye, Q.; Khan, M.U. Comparative study on three-dimensional statistical damage constitutive modified model of rock based on power function and Weibull distribution. *Environ. Earth Sci.* **2018**, *77*, 108. [CrossRef]
12. Hu, X.L.; Qu, S.J.; Li, K.Q. Study of rock elastoplastic constitutive damage model based on the unified strength theory. *J. China Univ. Min. Technol.* **2019**, *48*, 305–312.
13. Xie, S.J.; Han, Z.Y.; Chen, Y.F.; Wang, Y.X.; Zhao, Y.L.; Lin, H. Constitutive modeling of rock materials considering the void compaction characteristics. *Archiv. Civ. Mech. Eng.* **2022**, *22*, 60. [CrossRef]
14. Li, T.B.; Chen, Z.Q.; Chen, G.Q.; Ma, C.C.; Tang, O.L.; Wang, M.J. An experimental study of energy mechanism of sandstone with different moisture contents. *Rock Soil Mech.* **2015**, *36*, 229–236.
15. Zhao, G.M.; Liu, Z.X.; Meng., X.R.; Zhang, R.F.; Kao, S.M.; Qi, M.J. Minjie Energy accumulation and dissipation test and analysis method of height-diameter ratio sandstone. *J. China Coal Soc.* **2022**, *47*, 1110–1121.
16. Meng, Q.B.; Wang, C.K.; Huang, B.X.; Pu, H.; Zhang, Z.Z.; Sun, W.; Wang, J. Rock energy evolution and distribution law under triaxial cyclic loading and unloading conditions. *Chin. J. Rock Mech. Eng.* **2020**, *39*, 2047–2059.
17. Wu, Z.H.; Song, Z.Y.; Tan, J.; Zhang, Y.Z.; Qi, Z.J. The evolution law of rock energy under different graded cyclic loading and unloading modes. *J. Min. Saf. Eng.* **2020**, *37*, 836–844+851.
18. Li, X.W.; Yao, Z.S.; Huang, X.W.; Liu, Z.X.; Zhao, X.; Mu, K.H. Investigation of deformation and failure characteristics and energy evolution of sandstone under cyclic loading and unloading. *Rock Soil Mech.* **2021**, *42*, 1693–1704.
19. Zhang, T.; Liu, Y.; Yang, K.; Tang, M.; Yu, X.; Yu, F. Hydromechanical coupling characteristics of the fractured sandstone under cyclic loading-unloading. *Geofluids* **2020**, *2020*, 8811003. [CrossRef]
20. Srinivasan, V.; Gupta, T.; Ansari, T.A.; Singh, T.N. An experimental study on rock damage and its influence in rock stress memory in a metamorphic rock. *Bull. Eng. Geol. Environ.* **2020**, *79*, 4335–4348. [CrossRef]
21. Gajst, H.; Shalev, E.; Weinberger, R.; Marco, S.; Zh, W.; Lyakhovsky, V. Relating strain localization and kaiser effect to yield surface evolution in brittle Rocks. *Geophys. J. Int.* **2020**, *221*, 2091–2103. [CrossRef]
22. Becker, D.; Cailleau, B.; Dahm, T.; Shapiro, S.; Kaiser, D. Stress Triggering and stress memory observed from acoustic emission records in a salt mine. *Geophys. J. Int.* **2010**, *182*, 933–948. [CrossRef]
23. Zhao, B.Y.; Liu, D.Y.; Li, Z.Y.; Huang, W.; Dong, Q. Mechanical behavior of shale rock under uniaxial cyclic loading and unloading condition. *Adv. Civ. Eng.* **2018**, *2018*, 9750480. [CrossRef]
24. Xie, H.P.; Ju, Y.; Li, L.Y. Criteria for strength and structural failure of rocks based on energy dissipation and energy release principles. *Chin. J. Rock Mech. Eng.* **2005**, *24*, 3003–3010.
25. Xie, H.P.; Peng, R.D.; Ju, Y. Energy dissipation of rock deformation and fracture. *Chin. J. Rock Mech. Eng.* **2004**, *21*, 3565–3570.
26. Xie, H.P.; Ju, Y.; Li, L.Y.; Peng, R.D. Energy mechanism of deformation and failure of rockmasses. *Chin. J. Rock Mech. Eng.* **2008**, *27*, 1729–1740.
27. Miao, S.J.; Liu, Z.J.; Zhao, X.G.; Huang, Z.J. Energy dissipation and damage characteristics of Beishan granite under cyclic loading and unloading. *Chin. J. Rock Mech. Eng.* **2021**, *40*, 928–938.
28. Liu, Y.; Dai, F. A damage constitutive model for intermittent jointed rocks under cyclic uniaxial compression. *Int. J. Rock Mech. Min.* **2018**, *103*, 289–301. [CrossRef]
29. Cao, W.G.; Fang, Z.L.; Tang, X.J. A study of statistical constitutive model for soft and damage rocks. *Chin. J. Rock Mech. Eng.* **1998**, *17*, 628–633.
30. Cao, W.G.; Zhang, S. Study on the statistical analysis of rock damage based on Mohr- Coulomb criterion. *J. Hunan Univ. Nat. Sci.* **2005**, *32*, 43–47.
31. Cao, W.G.; Zhao, M.H.; Liu, C.X. Study on the model and its modifying method for rock softening and damage based on Weibull random distribution. *Chin. J. Rock Mech. Eng.* **2004**, *23*, 3226–3231.
32. Jiang, H. Expressing strength criterion in principalstress plane base on equivalent Mohr-Coulomb friction angle. *J. Cent. South Univ. (Sci. Technol.)* **2012**, *43*, 3216–3221.
33. Geng, N.G. Earthquakes caused by stress decreasing. *Acta Seismol. Sin.* **1985**, *7*, 445–451.
34. Geng, N.G.; Xu, D.J. Rock rupture caused by decreasing the minimum principal stress. *Chin. J. Geophys.* **1985**, *28*, 191–197.
35. Mogi, K. Fracture and flow of rocks under high triaxial compression. *J. Geophys. Res.* **1971**, *76*, 1255–1269. [CrossRef]
36. Mogi, K. Effect of the intermediate principal stress on rock failure. *J. Geophys. Res.* **1967**, *72*, 5117–5131. [CrossRef]
37. Al-Ajmi, A.M.; Zimmerman, R.W. Relation Between the Mogi and the Coulomb Failure Criteria. *Int. J. Rock Mech. Min. Sci.* **2005**, *42*, 432–439. [CrossRef]

Disclaimer/Publisher's Note: The statements, opinions and data contained in all publications are solely those of the individual author(s) and contributor(s) and not of MDPI and/or the editor(s). MDPI and/or the editor(s) disclaim responsibility for any injury to people or property resulting from any ideas, methods, instructions or products referred to in the content.